

1 Ink-jet printing versus solvent casting to prepare oral films: effect
2 on mechanical properties and physical stability

3

4 Asma B.M. Buanz, Claudia C. Belaunde, Nina Soutari, Catherine Tuleu, Mine Orlu
5 Gul and Simon Gaisford*

6 UCL School of Pharmacy, University College London, 29-39 Brunswick Square,
7 London, WC1N 1AX, UK.

8

9

10

11

12

13

14 * Corresponding author

15 Email: s.gaisford@ucl.ac.uk

16 Tel: +44(0) 207 753 5863

17 Fax: +44(0) 207 753 5942

18

19 **Abstract**

20

21 The aim of this work was to compare and contrast the mechanical properties and
22 physical stabilities of oral films prepared with either thermal ink-jet printing (TIJP) or
23 solvent casting (SC). Clonidine hydrochloride was selected as a model drug because
24 of its low therapeutic dose and films were prepared using cellulose polymers.

25 Mechanical testing showed that printed films had Young's moduli and tensile strength
26 values similar to the free film, while casted films were significantly more brittle. The
27 drug also appeared to crystallise out of casted films during stress testing whereas
28 printed films remained unchanged. The dissolution behaviour of printed and cast
29 films were similar, because of the rapid disintegration of the polymer. The conclusion
30 is that printing resulted in a better film than casting because the drug resided *on* the
31 film, rather than *in* the film where it could exert a plasticising effect.

32

33 **Key words**

34

35 Thermal inkjet printing, oral films, clonidine, dynamic mechanical analysis, critical
36 humidity.

37

38 **1. Introduction**

39 Oro-dispersible films (ODFs) have gained a lot of attention in recent years as a novel
40 technology to overcome some of the common issues associated with conventional
41 oral dosage forms, such as difficulty of swallowing (tablets and capsules) and stability
42 (solutions and suspensions) (Banbury and MacGregor, 2011; Jeong et al., 2010;
43 Saigal et al., 2008). ODFs are the size of a postage stamp and typically made from
44 good film-forming polymers that dissolve or disintegrate rapidly upon contact with
45 saliva (Banbury and MacGregor, 2011). They are flexible, which makes
46 transportation and consumer handling much easier (Borsadia et al., 2003), and their
47 manufacture can be cost effective (Reiner et al., 2010).

48
49 ODFs are not, however, without drawbacks. One is their limited drug loading
50 capacity, which makes them most suitable for highly potent, low-dose active
51 pharmaceutical ingredients (APIs). Other limitations include the need for solvents and
52 heat in the manufacturing process and the issue of taste masking. The main
53 formulation challenge is to produce films with a rapid disintegration/dissolution time
54 without compromising mechanical properties (Hoffmann et al., 2011).

55
56 Well-established technologies such as solvent casting (SC) and hot-melt extrusion
57 (HME) are used commercially to manufacture ODFs. In either case a polymer
58 network is produced that is cut into strips of the required size. Both methods require
59 the drug and the polymer to be mixed prior to forming the film. HME processing may
60 not be suitable for APIs that are thermally labile or are degraded following shear
61 stress (Janßen et al, 2013). One issue is that ODFs manufactured via these methods
62 are essentially solid amorphous dispersions, with the API molecularly dispersed in
63 the polymer matrix. It is well known that small molecular weight organic compounds
64 typically exert a plasticising effect on polymers, which means the mechanical
65 properties of the film may change depending on the amount and/or chemical

66 structure of the API incorporated. A further concern is that if the drug is formulated at
67 a super-saturated concentration, relative to its solubility in the polymer, it is likely to
68 phase separate by crystallising during storage. Crystallisation could potentially
69 change the mechanical properties of the film, alter the dissolution rate, change the
70 mouth feel and/or taste of the product and possibly alter the *in-vivo* fate of the drug
71 (Cespi et al., 2011).

72

73 An alternative route of manufacture is to cast a free film and then deposit the API
74 onto it. One approach is to use flexography (a contact printing method that uses
75 rotating rollers to deposit the printing solution onto the substrate). Genina et al (2012)
76 used flexographic printing to formulate films for controlled release while Janßen et al
77 (2013) used flexography to dispense rasagiline mesylate solution and tadalafil
78 suspension onto hydroxypropylmethylcellulose films. Incorporation of
79 hydroxypropylcellulose seemed to reduce drug crystallisation after printing. However,
80 the main limitations of flexography are the risk of contamination, the relatively low
81 resolution and the need to prepare a print roller, which means it is most suited to
82 medium-scale production runs (Gonzalez-Macia et al., 2010).

83

84 The API may also be deposited with thermal inkjet printing (TIJP). TIJP has the
85 advantage of being able to deposit very small volumes (5-15 pL per droplet) with high
86 precision. We have demonstrated before the deposition of low doses of salbutamol
87 sulphate onto commercially available starch-based films with using conventional
88 desktop printers (Buanz et al., 2011). TIJP technology has also been used to
89 manufacture modified-release dosage forms by printing dots of solution onto a
90 substrate (Scoutaris et al 2011, 2012) and it has been shown possible to fabricate
91 three-dimensional particles by printing aqueous droplets into liquid nitrogen and
92 subsequently freeze-drying (Mueannoorn et al, 2012; Sharma et al, 2013).

93

94 Since TIJP deposits API solution *onto* a substrate, rather than dispersing API *within* a
95 substrate, it seems reasonable to assume that printed films would maintain
96 mechanical properties similar to that of the free film, and hence offer potential
97 benefits compared with solvent casting for ensuring long-term stability. Testing this
98 hypothesis is the specific aim of this work. Clonidine (CLN) was selected as a model
99 drug. Clonidine is an antihypertensive drug that acts centrally by blocking α_2 -
100 adrenoreceptors. It also has sedative and analgesic effects (Ambrose et al., 2000).
101 The drug is available as tablets of 100 and 300 μg as the chloride salt (Paediatric
102 Formulary Committee, 2011) and the required dose to induce pre-operative sedation
103 is 1- 5 $\mu\text{g}/\text{kg}$ (Bergendahl et al., 2006). Such low doses make CLN an ideal candidate
104 for formulation as oral films.

105

106 **2. Materials and methods**

107 2.1 Materials

108 CLN, polyvinyl alcohol (PVA) 98% hydrolysed (Mw 13000-23000) and
109 carboxymethylcellulose sodium salt medium viscosity (SCMC) were purchased from
110 Sigma Aldrich (UK). Glycerol (analytical grade) was purchased from Fischer
111 Scientific (UK). Bidistilled water (99.5%) was purchased from VWR International Ltd
112 (UK), and methanol, absolute ethanol and acetonitrile (HPLC grade) were all
113 purchased from Fischer Scientific (UK). Sodium 1-hexanesulphate (99%) was
114 purchased from Acros organics (USA).

115

116 2.2 Film preparation

117 Films were prepared either by solvent casting or ink-jet printing. Concentrations were
118 based on the minimum and maximum doses for sedation for children aged 6 months,
119 5 and 14 years (Table 1).

120

121 2.2.1 Printed films

122 The free film was composed of PVA and SCMC at 1:1 ratio with 24%w/v glycerol
123 (Soutari et al, 2012). PVA (3.75g) was first dissolved in water (about 100mL) by
124 heating to 80°C with continuous stirring. SCMC (3.75g) was then added and the
125 solution was left to cool to room temperature with mixing, following which glycerol
126 was added (36g) and the final volume was adjusted to 150mL with water. The solution
127 was poured into a non-stick baking tray (450cm²) and dried in an oven at 30°C. The
128 resulting film sheets were used as substrates for printing.

129

130 An HP printer (HP Deskjet 460, Hewlett-Packard Inc.) was used to print drug solution
131 onto the film. Solutions of CLN (50mg/mL, prepared in 20% v/v methanol in water
132 with 10%v/v glycerol) were printed from an HP 338 black cartridge. The cartridge was
133 prepared by cutting off the top, removing the ink and rinsing with absolute ethanol. A
134 2cm x 2cm black template was created in Word 2007 (Microsoft Inc., USA) and used
135 to fire the cartridge. It was found that per print pass, 316.0 µg of CLN were deposited
136 per strip (4cm²), equivalent to 79.0 µg/cm². This value was then used to prepare CLN
137 solutions suitable for printing films with doses equivalent to those given in Table 1.

138

139 2.2.2 Casted films

140 Appropriate volumes of CLN solutions (3.3, 1.18, 0.66, 0.5, 0.24 and 0.1 mg/mL to
141 prepare 250, 90, 50, 38, 18 and 7.6 µg/strip, respectively) were added to a
142 PVA:SCMC solution (prepared as above) to obtain the required dose. Solutions were
143 left to stir for one hour and then were cast in a non-stick baking tray and dried at
144 30°C. The resulting films were cut to the required size (4 cm²) and stored over silica
145 gel in a desiccator until use.

146

147 2.3 Drug content analysis

148 Films were dissolved in a solution of 20% methanol in water (4 cm² in 20 mL).
149 Solutions were filtered through a 0.45 µm filter (Millex syringe-driven filter unit,
150 Millipor Ltd, Ireland). The filtrate was analysed with high performance liquid
151 chromatography (HPLC) equipped with a UV-diode-array detector (Agilent
152 Technologies 1200 series, Germany). The mobile phase was a mixture of 0.1% v/v
153 trifluoroacetic acid in water and acetonitrile (80:20% v/v) delivered at a rate of 1.0
154 mL/min. The stationary phase was a Phenomenex Synergy max C-12 column
155 (250mm x 4.6mm x 4µm; Phenomenex Synergy max, USA) kept at 40°C and the
156 injected sample volume was 10µL. Peaks were evaluated at 220nm. The percentage
157 recovery calculated for solutions made with blank film sheets dissolved in the
158 solutions spiked with known amount of CLN (in the range of 100 to 300 µg/mL, n=9)
159 was 98.29 ± 1.82%. Limit of detection and limit of quantification were found to be
160 0.15µg/mL and 0.68µg/mL, respectively. Method calibration was performed with a
161 series of standard CLN solutions in 20% methanol in water. A linear response was
162 seen between 0.25 and 100 µg/mL ($r^2 = 0.9997$).

163

164 2.4 Characterisation of films

165 2.4.1 X-Ray Powder Diffraction (XRPD)

166 Powder diffraction data were collected with a PW3830 diffractometer (Philips,
167 Netherlands) operated with Cu K-alpha radiation ($\lambda = 1.540598 \text{ \AA}$) at 45 kV and 30
168 mA. Scanning was performed from 5° to 30° 2θ at 0.02° step size and 2.85 seconds
169 per step. Xpert data viewer software (PANalytical B.V, Netherland) was used to
170 analyse the data.

171

172 2.4.2 Thermogravimetric analysis (TGA)

173 Measurements were performed with a Pyris-6 TGA (PerkinElmer, UK). Samples were
174 heated at 10°C/min using nitrogen as purge gas (20mL/min). Data collection and

175 analysis were performed using Pyris software (version 3.18). Mass loss (%w/w)
176 and/or onset temperature were calculated and reported as mean \pm SD.

177

178 2.4.3 Fourier Transform Infrared (FTIR)

179 FTIR spectra were collected with a PerkinElmer Spectrum 100 FTIR spectrometer in
180 the range of 4000 to 650 cm^{-1} at ambient conditions. Spectra were analysed with
181 Spectrum Express software (application version 1.02.00.0014, 2008).

182

183 2.4.4 Tensile testing

184 An Instron Universal Testing Instrument (Model 5567, Instron Ltd, Norwood, USA)
185 was used to measure the mechanical properties of films (2cm x 2cm) at a rate of
186 10mm/min and 100N static load (2kg). The cut-off point was when the film was
187 completely separated into two pieces. The tensile strength and Young's modulus
188 were measured. Data were analysed using Bluehill software 2 (version 2.6).

189

190 2.4.5 Dynamic Mechanical Analysis (DMA)

191 A Q800 Dynamic Mechanical Analyser (TA instruments, Waters LLC) was used to
192 measure the mechanical properties of the films. Advantage software for Q series
193 version 2.8.0.394 was used to collect the data and TA Universal Analysis software
194 (V4. 7A TA 2000) to analyse the data. Samples were held in a film tension clamp.
195 Experimental parameters were amplitude, 15-20 μm ; preforce load, 0.01N; force
196 track, 125%; frequency, 10Hz. Experiments were performed at 3°C/min from room
197 temperature to 200°C.

198

199 2.4.6 Polarised light microscopy (PLM)

200 A Nikon microphot-FXA light microscope was used to collect optical images with an
201 Infinity 2 digital camera and capture application software (version 3.7.5).

202

203 2.4.7 Dynamic Vapour Sorption (DVS)

204 Films were placed in a glass pan for Dynamic Vapour Sorption (DVS-1) (Surface
205 Measurement Systems, London, UK) at 30°C and kept at 0% RH for 90 minutes.
206 Relative humidity was then scanned from 0 to 95% with intervals of 5% RH over 10
207 minutes. The change of sample weight due to water uptake or loss was recorded
208 gravimetrically with the ultra-microbalance. The relative humidity (RH) around the
209 sample was controlled by mixing saturated and dry carrier gases (Nitrogen) with
210 electronic mass flow controllers.

211

212 2.4.8 Thickness and disintegration

213 Thickness of films (2cm x 2cm) was measured using a digital micrometer at five
214 points of each sample, at the four corners and the centre in triplicate, and reported as
215 mean \pm SD.

216

217 The disintegration test described by Zhao et al (2009) for capsule and tablet coatings
218 was modified to suit oral films. A device was constructed to hold the film between two
219 clamps and a weight of 725mg was placed on top of the film. The disintegration
220 medium used was 15 mL (37 ± 1 °C) of a simulated saliva solution (Peh and Wong,
221 1999) containing Na₂HPO₄ (2.38 g), KH₂PO₄ (0.19 g) and NaCl (8 g) in distilled water
222 (1 L). The pH of the solution was adjusted to 6.75 with phosphoric acid. The time
223 taken for the film to break was measured by filming with a black and white CCD
224 camera (model ART-CAM-130MI-VM). Images were analysed with FTA 32 software
225 (Version 2.0, First Ten Angstroms Inc, USA). The disintegration time was calculated
226 as the time between adding the disintegration medium and visual observation of the
227 film breaking (n = 3).

228

229 2.4.9 *In vitro* drug release

230 Dissolution tests were conducted in a water-jacketed glass vessel (outer and inner
231 diameters of 8 and 6 cm, respectively and 150mL capacity). Films were placed on a
232 plastic sieve of 3cm in diameter and 40 mL of simulated saliva solution was used as
233 a dissolution medium. A PTFE magnetic stirrer was used for agitation (size of 10cm x
234 6cm) and the temperature was maintained at 37 ± 1 °C with the help of a
235 refrigerating/heating circulator with programmable digital temperature controller
236 (Polyscience, Division of Preston Industries, Inc., USA). Samples of 1mL were
237 collected at time intervals of 0.5, 1, 2, 4, 8, 12, 16 and 30 min and replaced with a
238 fresh medium kept at ~ 37 °C. Samples were then filtered through 0.45 μ m filters and
239 analysed with HPLC in accordance with the method above.

240

241 2.5 Statistical analysis

242 Results were analysed and compared with Student t-test ($\alpha=0.05$) using Origin® 8.6
243 software (OriginLab Corporation, USA).

244

245 **3. Results and discussion**

246

247 3.1 Drug content and dose uniformity

248 The amount of CLN deposited by printing showed a linear correlation with the drug
249 feed solution concentration as shown in Figure 1 ($r^2 = 0.9997$). This is consistent with
250 the salbutamol sulphate (SS) data reported in an earlier study (Buanz et al, 2011).

251 Films prepared by blending CLN with the polymer and casting had a lower drug
252 content than films prepared by printing (Table 2). The variation of dose was higher
253 with solvent casting method ($CV= 10.8 \pm 6.0\%$) compared with printing ($CV= 2.5 \pm$
254 2.2%). The higher dose variability in casted films may be a result of inhomogeneity in
255 blending or variability in film thickness, but the results immediately indicate the

256 potential utility of ink-jet printing for preparing low dose and narrow therapeutic index
257 medicines.

258

259 3.2 Characterisation of films

260 In general, pharmaceutical polymer films should have good flexibility, elasticity and
261 softness but possess enough strength to withstand mechanical stresses during
262 manufacturing and dispensing (Preis et al., 2013; Prodduturi et al., 2004). Hydrophilic
263 polymers are commonly used in pharmaceutical oral dosage forms (Prodduturi et al.,
264 2004), which generally means that exposure to humidity during storage and use can
265 affect their properties (Gontard and Ring, 1996). Here, mechanical testing and
266 polarised-light microscopy were used to characterise the films after manufacture and
267 following exposure to elevated humidity.

268

269 3.2.1 Tensile test

270 Tensile stress at the break point and Young's modulus were calculated for drug-
271 loaded films (Table 3). Films prepared by SC had higher tensile stress values, which
272 indicates that the films were harder than those made by TIJP (Garsuch and
273 Breitzkreutz, 2010). Skulason et al (2009) reported that Carpalol films prepared by
274 SC have high tensile strength and low elasticity. In general, higher Young's modulus
275 values for films made by SC also reflect their increased brittleness (Biliaderis et al.,
276 1999).

277

278 Residual water in films can affect their mechanical properties and lead to increased
279 elasticity by its plasticizing effect (Karisson and Singh, 1998) and thus any variation
280 in water content between films prepared by TIJP and SC could be the reason for the
281 difference in their mechanical properties. However, as shown by values of water
282 content given in Table 3, the difference was not significant ($p > 0.05$). This suggests
283 that location of drug within the films is in fact the critical factor.

284

285 3.2.2 Glass transition measurement

286 XRPD patterns shown in Figure 2 confirm the amorphous nature of the free and
287 drug-loaded films. The glass transition temperature (T_g) of a polymer is one of the
288 important parameters that reflects its mechanical properties with temperature and is
289 associated with a small change in the heat capacity of the system due to the strong
290 glass forming properties of polymers (Fadda et al., 2010). There is no single
291 temperature at which T_g occurs; rather, the value depends on the technique and
292 experimental parameters used to measure it.

293

294 DMA was used to measure the glass transition temperatures of the films. T_g is
295 usually defined as a peak in the tan delta signal (the ratio of the storage to loss
296 moduli) or the inflection point of the decrease in storage modulus (Gontard and Ring,
297 1996). Here, it was not possible to use either point. The storage modulus data are
298 shown in Figure 3. It is apparent that there is an increase in storage modulus after
299 100 °C. This is because the films lost water during heating and so became very
300 brittle. Similarly, there was no peak in the tan delta signal (data not shown) because
301 the polymers thermally degraded. This highlights one significant problem when using
302 thermal methods at slow heating rates. The increase in temperature acts to dry the
303 sample and since water is often a plasticiser the mechanical properties of the film
304 change during measurement. Hence, it was not possible to determine the T_g values
305 of the films.

306

307 FTIR data, however, did show evidence of CLN-polymer interactions at room
308 temperature (Table 4). Shifts are noticeable in the bands at 3274.8 (broad), 2941.6
309 and 1380.5 (from the free film) in the drug-loaded films, which can be assigned to
310 hydroxyl (OH) stretch, and carbon-hydrogen (C-H) stretch and C-H bend,
311 respectively (Coates, 2000), suggesting that the drug interacts with PVA but not with

312 SCMC, possibly through hydrogen bond with the PVA OH group. Larger shifts from
313 the free film values are seen in the case of SC samples, indicating the drug is more
314 dispersed in the polymer matrix than in the printed films. It is noticeable that the main
315 bands characteristic for CLN, such as the secondary amine N-H stretch, bend and
316 aliphatic secondary amine C-N stretch (at 3330, 1649 and 1338) are not seen, which
317 could be because they are masked by peaks from the polymers or because the drug
318 concentration is very low.

319

320 3.2.3 Critical humidity measurement

321 The critical humidity (cRH) is the humidity at a particular temperature that will cause
322 a phase transition (such as glass transition). Its determination is important along with
323 the threshold temperature in order to define the storage conditions required to
324 prevent phase changes during processing and storage (Burnett et al., 2004).

325

326 DVS is commonly used to determine cRH. cRH is usually taken to be the RH where a
327 reduction in mass is seen, corresponding to expulsion of absorbed water as the
328 sample crystallises. For CLN films the sample weight continued to increase with a
329 increasing of RH (Figure 4), and so it was not possible to determine a cRH value.
330 Presumably, this is because the majority of the sample is polymer. The method of
331 preparation (TIJP or SC) did not seem to have an effect on water sorption at lower
332 humidity as the changes of weight with time (and humidity) of both samples appear to
333 be superimposed. However, at higher humidity a higher weight increase is observed
334 for printed films. Possible reasons for this difference are discussed below.

335

336 3.2.4 Physical stability

337 Stability here refers to physical form rather than chemical degradation. Upon
338 exposure to increased temperature and/or humidity the films may absorb water and

339 be plasticised thus increasing the rate of molecular mobility of dispersed drug
340 molecules and potentially causing phase separation by crystallisation.
341
342 Films containing the highest doses of CLN (90 and 250 µg/strip) were subjected to
343 high temperature and humidity (60°C and 75 %RH) in the DMA for about 13 hours.
344 The DMA signal (storage modulus) did not change after initial equilibration to the test
345 parameters. This indicates that there was no significant change in the mechanical
346 properties of the films over the test period. However, PLM images (Figure 5) showed
347 clear signs of crystallisation in the 250 µg/strip prepared by SC. No such
348 crystallisation was observed for the lower dose film prepared by SC or films prepared
349 by TIJP.

350
351 In addition, the films used during the DVS and DMA experiments were also checked
352 with PLM (Figure 6). These films were exposed to relative humidity from 0 to 90% RH
353 at 30°C. No signs of crystallisation can be seen in films tested with DMA but clear
354 crystallisation is evident in the 250 µg/strip films prepared by SC tested with DVS and
355 the beginning of crystal growth is seen in the 90 µg/strip films. Drug in films prepared
356 by TIJP showed no evidence of crystallisation.

357

358 3.2.1 Disintegration and drug release

359 Typical disintegration times for ODFs range from 5 to 30 s (Banhart, 2008). There
360 have been several attempts to mimic *in vivo* conditions, particularly the low volume of
361 saliva, such as the slide frame method and the Petri dish method (Garsuch and
362 Breitzkreutz, 2010; Hoffmann et al., 2011). Measurement of the contact angle with
363 time as a drop of water is placed on a film has also been used to assess
364 disintegration (Garsuch and Breitzkreutz, 2009). The lack of official tests makes the
365 comparison between various published results a challenging task.

366

367 Here, the images for film disintegration were captured with the help of a CCD
368 camera, allowing precise time measurement. For the dissolution test a volume of 40
369 mL was the lowest that allowed the film (placed on the plastic mesh) to float freely
370 while the medium was mixed. The results of both tests are described below.

371

372 The results from the disintegration test show that the time taken for the samples to
373 disintegrate is in the range of 20 to 60 s (the time recommended by the FDA is 30 s,
374 Centre for Drug Evaluation and Research, 2008). This means that some samples
375 exceeded the recommended limit. The main factor for that would be the thickness as
376 it is a key factor in determining the disintegration time (Garsuch and Breitzkreutz,
377 2010).

378

379 Figure 7 shows the release profiles of films containing 250 µg/strip of CLN prepared
380 by either TIJP or casting (SC) in simulated saliva fluid. It is noticeable that both
381 samples achieved more than 50% ($t_{50\%}$) and 80% ($t_{80\%}$) of drug release within 8 and 30
382 min, respectively. To compare the release profiles of films prepared by TIJP with
383 films prepared by SC, difference (f_1) and similarity (f_2) factors were calculated from
384 equations 1 and 2 ($n = 3$). f_2 can have a value of 0 to 100 where 100 means the
385 profile of the tested product is the same as that of the reference and 0 means they
386 are completely different (Costa and Sousa Lobo, 2001). The FDA adopted both
387 factors as a way to assess the similarity of *in vitro* dissolution profiles where a value
388 of 0 to 15 for (f_1) and 50 to 100 for (f_2) indicate the two profiles to be similar (Center
389 for Drug Evaluation and Research, 1997). f_1 and f_2 for films containing 250 µg/strip
390 prepared by TIJP were calculated to be 1.25 and 64.7, respectively, which means
391 that the release profile of TIJP films is similar to that of films prepared by SC.

392

393 $f_1 = \{[\sum_{t=1}^n (R_t - T_t)] / [\sum_{t=1}^n R_t]\} \times 100$ **Equation 3.1**

$$394 \quad f_2 = 50 \log \left\{ \left[1 + \frac{1}{n} \sum_{t=1}^n (R_t - T_t)^2 \right]^{-0.5} \right\} \times 100 \quad \text{Equation 3.2}$$

395

396 Where n is the number of data points and R and T are the cumulative release
 397 percentages for the reference (SC) and the test (TIJP) films at time t .

398 The release kinetics of CLN from the films were examined with four mathematical
 399 release models; zero-order, first-order, Higuchi and Hixson-Crowell models
 400 (Equations 3 to 6) (Costa and Sousa Lobo, 2001). Where Q_t and Q_0 are the amount
 401 released after time t and initial amount of the drug, respectively while k is the release
 402 constant.

403

$$404 \quad Q_t = Q_0 + Kt \quad \text{Equation 3}$$

$$405 \quad \ln Q_t = \ln Q_0 + Kt \quad \text{Equation 4}$$

$$406 \quad Q_t = K\sqrt{t} \quad \text{Equation 5}$$

$$407 \quad Q_t^{1/3} = Q_0^{1/3} + Kt \quad \text{Equation 6}$$

408

409 The correlation coefficients (r^2) for films prepared by TIJP or SC are given in (Table
 410 5). The highest r^2 value was for Hixson-Crowell model. This suggests that drug
 411 release from both samples followed this model, which indicates drug release by
 412 erosion (Costa et al., 2003). This could be a result of incorporating SCMC in the
 413 formulation (Dabbagh et al., 1999; Hussain et al., 1994). This could be related to the
 414 presence of ionisable carboxylic acid group in SCMC, which increases the dissolution
 415 of the polymer (Hussain et al., 1994). Dabbagh et al (1999) noticed a decrease in
 416 matrix erosion when propranolol hydrochloride was added, which they suggested to
 417 be a result of an interaction between the drug and the polymer. In this work the FTIR
 418 data presented earlier suggest that clonidine hydrochloride interacts with PVA and
 419 not SCMC in the tested films. This supports the suggestion that the carboxylic acid
 420 groups of SCMC are available for ionisation and thus allows the polymer erosion.

421 Hussain et al (1994) also reported that when comparing the erosion rate of SCMC
422 matrices containing either a drug that interacts with the polymer or not, a faster rate
423 is observed when no interaction is present.

424

425 **4. Conclusion**

426 The results indicate that films prepared by printing are significantly different in terms
427 of mechanical properties and stability compared with films prepared by casting. In
428 particular, the properties of the printed films are much more similar to those of the
429 free film. It seems likely that the process of solvent casting results in a molecular
430 dispersion of CLN throughout the polymer, analogous to a solid-amorphous
431 dispersion. FTIR data confirm chemical interaction between the drug and the
432 polymer. The drug appears to exert an anti-plasticising effect, increasing the
433 brittleness of the film. When stored at elevated temperature and humidity the drug is
434 seen to phase separate, resulting in crystal formation.

435

436 The exact nature of the printed film is harder to elucidate from the data. It is clear that
437 immediately after printing the drug will be present in solution as droplets on the
438 surface of the polymer film. Previous experience with printing drug solutions (Buanz
439 et al, 2013) has shown us that the small droplets evaporate very quickly, resulting in
440 formation of small (<5 μm) crystals. Thus, a reasonable hypothesis would be that in
441 the printed films the drug exists either on the surface or in the top layer of the film as
442 small crystallites. The drug is thus not acting as an anti-plasticiser and so the
443 mechanical properties of the printed film remain similar to those of the free film. The
444 printed film appears amorphous by XRPD because the drug content is low and small
445 crystals do not diffract sufficiently to appear in the pattern. Upon storage at elevated
446 temperature and humidity the printed film remains stable because it has already
447 phase separated. Again, it is likely that the small size of any crystallites mean they
448 were not visible with PLM.

449

450 Janßen et al (2013) did not observe any effect on the mechanical properties of films
451 upon printing drug solutions using flexographic printing. They argue that in
452 manufacturing oral films by this method the properties of the plain films can be
453 assessed and it would not be necessary to evaluate the medicated films, which they
454 envisage to add flexibility to the manufacturing process. Our work indicates a similar
455 conclusion can be drawn in regard to ink-jet printing.

456

457

458 **5. References**

- 459 Ambrose, C., Sale, S., Howells, R., Bevan, C., Jenkins, I., Weir, P., Murphy, P. and
460 Wolf, A., 2000. Intravenous clonidine infusion in critically ill children: Dose-dependent
461 sedative effects and cardiovascular stability. *Br. J. Anaesth.* 84, 794-796.
- 462 Banbury, S., MacGregor, K., 2011. Fast-dispersing dosage forms for the pediatric
463 market. *Drug Delivery Tech.* 11, 32-35.
- 464 Banhart, S.D., 2008. Thin film oral dosage forms. *Modified-release drug delivery*
465 *technology*. In, Rathbone, M., Hadgraft, J. and Roberts, M., Informa Healthcare.
466 Volume 1: 209-216. ISBN: 1-4200-4435-4.
- 467 Bergendahl, H., Lönnqvist, P.A., Eksborg, S., 2006. Clonidine in paediatric
468 anaesthesia: Review of the literature and comparison with benzodiazepines for
469 premedication. *Acta Anaesth. Scand.* 50, 135-143.
- 470 Biliaderis, C.G., Lazaridou, A., Arvanitoyannis, I., 1999. Glass transition and physical
471 properties of polyol-plasticised pullulan-starch blends at low moisture. *Carbo. Pol.* 40,
472 29-47.
- 473 Borsadia, S., O'Halloran, D., Osborne, J., 2003. Quick-dissolving films- a novel
474 approach to drug delivery. *Drug Dev. Del.* 3, 63-66.
- 475 Buanz, A.B.M., Saunders, M.H., Basit, A.W., Gaisford, S., 2011. Preparation of
476 personalized-dose salbutamol sulphate oral films with thermal ink-jet printing. *Pharm.*
477 *Res.* 28, 2386-2392.
- 478 Buanz, A.B.M., Telford, R., Scowen, I.J., Gaisford, S. 2013. Rapid preparation of
479 pharmaceutical co-crystals with thermal ink-jet printing. *CrystEngComm.* 15, 1031-
480 1035.
- 481 Burnett, D.J., Thielmann, F., Booth, J., 2004. Determining the critical relative humidity
482 for moisture-induced phase transitions. *Int. J. Pharm.* 287, 123-133.
- 483 Center for Drug Evaluation and Research (CEDR). 2008. Guidance for industry orally
484 disintegrating tablets. U.S. Department of Health and Human Services U.S. Food and
485 Drug Administration

486 Cespi, M., Bonacucina, G., Mencarelli, G., Casettari, L., Palmieri, G.F., 2011.
487 Dynamic mechanical thermal analysis of hypromellose 2910 free films. Eur. J.
488 Pharm. Biopharm. 79, 458-463.

489 Coates, J., 2000. Interpretation of infrared spectra, a practical approach.
490 *Encyclopedia of analytical chemistry*. Meyers, R. A. Chichester, John Wiley & Sons
491 Ltd: 10815-10837.

492 Costa, P., Sousa Lobo, J.M., 2001. Modeling and comparison of dissolution profiles.
493 Eur. J. Pharm. Sci. 13, 123-133.

494 Costa, F.O., Sousa, J.J.S., Pais, A.A.C.C., Formosinho, S.J., 2003. Comparison of
495 dissolution profiles of ibuprofen pellets. J. Cont. Rel. 89, 199-212.

496 Dabbagh, M.A., Ford, J.L., Rubinstein, M.H., Hogan, J.E., Rajabi-Siahboomi, A.R.,
497 1999. Release of propranolol hydrochloride from matrix tablets containing sodium
498 carboxymethylcellulose and hydroxypropylmethylcellulose. Pharm. Dev. Tech. 4,
499 313-324..

500 Fadda, H.M., Khanna, M., Santos, J.C., Osman, D., Gaisford, S., Basit, A.W., 2010.
501 The use of dynamic mechanical analysis (DMA) to evaluate plasticization of acrylic
502 polymer films under simulated gastrointestinal conditions. Eur. J. Pharm. Biopharm.
503 76, 493-497.

504 Garsuch, V., Breitzkreutz, J., 2009. Novel analytical methods for the characterization
505 of oral wafers. Eur. J. Pharm. Biopharm. 73, 195-201.

506 Garsuch, V., Breitzkreutz, J., 2010. Comparative investigations on different polymers
507 for the preparation of fast-dissolving oral films. J. Pharm. Pharmacol. 62, 539-545.

508 Genina, N., Fors, D., Vakili, H., Ihalainen, P., Pohjala, L., Ehlers, H., Kassamakov, I.,
509 Haeggström, E., Vuorela, P., Peltonen, J., Sandler, N., 2012. Tailoring controlled-
510 release oral dosage forms by combining inkjet and flexographic printing techniques.
511 Eur. J. Pharm. Sci. 47, 615-623.

512 Gontard, N., Ring, S., 1996. Edible wheat gluten film: Influence of water content on
513 glass transition temperature. J. Agr. Food Chem. 44, 3474-3478.

514 Gonzalez-Macia, L., Morrin, A., Smyth, M.R., Killard, A.J., 2010. Advanced printing
515 and deposition methodologies for the fabrication of biosensors and biodevices.
516 Analyst 135, 845-867.

517 Hoffmann, E.M., Breitenbach, A., Breitzkreutz, J., 2011. Advances in orodispersible
518 films for drug delivery. Exp. Opin. Drug Del. 8, 299-316.

519 Hussain, A.S., Johnson, R.D., Shivanand, P., Zoglio, M.A., 1994. Effects of blending
520 a nonionic and an anionic cellulose ether polymer on drug release from hydrophilic
521 matrix capsules. Drug Dev. Ind. Pharm. 20, 2645-2657.

522 Janßen, E.M., Schliephacke, R., Breitenbach, A., Breitzkreutz, J., 2013. Drug-printing
523 by flexographic printing technology—a new manufacturing process for orodispersible
524 films. Int. J. Pharm. 441, 818-825.

525 Jeong, S.H., Lee, J., Woo, J.S., 2010. Fast disintegrating tablets. In, Oral controlled
526 release formulation design and drug delivery, John Wiley & Sons, Inc.: 155-167.

527 Karisson, A., Singh, S.K., 1998. Thermal and mechanical characterization of
528 cellulose acetate phthalate films for pharmaceutical tablet coating: Effect of humidity
529 during measurements. Drug Dev. Ind. Pharm. 24, 827-834.

530 Mueannoorn, W., Srisongphan, A., Taylor, K.M.G., Hauschild, S., Gaisford, S., 2012.
531 Thermal ink-jet spray freeze-drying for preparation of excipient-free particles of
532 salbutamol sulphate for inhalation. Eur. J. Pharm. Biopharm. 80, 149-155.

533 Paediatric Formulary Committee 2011. British National Formulary for Children.
534 London, BMJ Group, Pharmaceutical Press, and RCPCH Publications.

535 Peh, K.K., Wong, C.F., 1999. Polymeric films as vehicle for buccal delivery: Swelling,
536 mechanical, and bioadhesive properties. J. Pharm. Pharm. Sci. 2, 53-61.

537 Preis, M., Woertz, C., Kleinebudde, P., Breitzkreutz, J., 2013. Oromucosal film
538 preparations: Classification and characterization methods. Exp. Opin. Drug Del.
539 10(9): 1-15.

540 Prodduturi, S., Manek, R.V., Kolling, W.M., Stodghill, S.P., Repka, M.A., 2004. Water
541 vapor sorption of hot-melt extruded hydroxypropyl cellulose films: Effect on physico-

542 mechanical properties, release characteristics, and stability. J. Pharm. Sci. 93. 3047-
543 3056.

544 Reiner, V., Giarratana, N., Monti, N.C., Breitenbach, A., Klaffenbach, P., 2010.
545 Rapidfilm®: An innovative pharmaceutical form designed to improve patient
546 compliance. Int. J. Pharm. 393, 55-60.

547 Saigal, N., Baboota, S., Ahuja, A., Ali, J., 2008. Fast-dissolving intra-oral drug
548 delivery systems. Exp. Opin. Therapeu. Pat. 18, 769-781.

549 Scoutaris, N., Alexander, M.R., Gellert, P.R., Roberts, C.J., 2011. Inkjet printing as a
550 novel medicine formulation technique. J. Cont. Rel. 156, 179-185.

551 Scoutaris, N., Hook, A.L., Gellert, P.R., Roberts, C.J., Alexander, M.R., Scurr, D.J.,
552 2012. ToF-SIMS analysis of chemical heterogeneities in inkjet micro-array printed
553 drug/polymer formulations. J. Mater. Sci. Mater. Med. 23, 385-391.

554 Sharma, G., Mueannoom, W., Buanz, A.B.M., Taylor, K.M.G., Gaisford, S., 2013. In
555 vitro characterization of terbutaline sulphate particles prepared by thermal ink-jet
556 spray freeze drying. Int. J. Pharm. 447, 165-170.

557 Skulason, S., Asgeirsdottir, M.S., Magnusson, J.P., Kristmundsdottir, T., 2009.
558 Evaluation of polymeric films for buccal drug delivery. Pharmazie 64, 197-201.

559 Soutari, N., Buanz, A.B.M., Orlu Gul, M., Tuleu, C., Gaisford, S., 2012. Quantifying
560 crystallisation rates of amorphous pharmaceuticals with dynamic mechanical analysis
561 (DMA). Int. J. Pharm. 423, 335-340.

562 Zhao, J., Gaynor, S., Schmitt, B., Coppens, K., Spaulding, W., 2009. Mechanical,
563 permeation and disintegration behavior of films based on hypromellose and its
564 blends. *2009 Annual Meeting and Exposition of the American Association of*
565 *Pharmaceutical Scientists*. Los Angeles, California.

566

567

568

Age/Body weight	Target dose ($\mu\text{g}/\text{strip}$)	Required feed solution conc. (mg/mL)
6 months/7.6Kg	7.6	1.20
	38	2.85
5 year-old/18Kg	18	6.01
	90	7.91
14-year old/ 50Kg	50	14.23
	250	39.54

569

570 **Table 1. Clonidine hydrochloride doses and the required solution**

571 **concentrations used for depositing the drug by TIJP.**

572

Target conc. (µg/strip)	Calculated Concentration (µg/strip)					
	SC (weight-based)		SC (area-based)		TIJP (area-based)	
	Mean ± SD	% Difference	Mean ± SD	% Difference	Mean ± SD	% Difference
7.6	9.9 ± 1.3	30.1 ± 17.4	10.6 ± 0.5	39.1 ± 6.5	12.2 ± 0.4	60 ± 5.0
18	26.0 ± 2.6	44.3 ± 14.3	18.6 ± 1.0	3.5 ± 5.8	19.1 ± 1.1	5.9 ± 5.9
38	31.1 ± 15.0	-18.3 ± 39.5	30.3 ± 6.5	-20.3 ± 17	36.5 ± 1.7	-4 ± 4.4
50	51.8 ± 2.3	3.6 ± 4.5	42.7 ± 4.3	-14.7 ± 8.5	45.9 ± 0.1	-8.1 ± 0.3
90	116.7 ± 43.5	29.4 ± 48.3	73.5 ± 8.4	-18.3 ± 9.3	80.4 ± 0.4	-10.7 ± 0.4
250	226.7 ± 5.8	-9.3 ± 2.3	203.9 ± 23.9	-18.4 ± 9.6	252.8 ± 2.5	1.1 ± 1

573

574 **Table 2. A comparison between drug content in films prepared by SC and TIJP**

575 **methods.**

576

577

Sample	Free film	250 µg/strip	
		SC	TIJP
Tensile stress (MPa)	19.3 ± 2.9	41.9 ± 1.9	25.2 ± 1.1
Young's modulus (MPa)	547.8 ± 54.2	1423.8 ± 259.1	658.2 ± 127.6
Water content (%w/w)	8.9 ± 0.1	5.8 ± 0.3	6.6 ± 1.1
Thickness (mm)	0.1 ± 0.02	0.1 ± 0.01	0.1 ± 0.01
Disintegration time (seconds)	NA	23.3 ± 5.6	30.5 ± 4.6

578

579 **Table 3. Mechanical properties, water content, thickness and disintegration**
580 **times for films prepared by SC or TIJP methods.**

581

582

Sample	TIJP 250 µg/strip	SC 250 µg/strip	Free film	PVA powder	SCMC powder	CLN powder
Wavelength (cm ⁻¹)	3276.4	3270.8	3274.8	3278.7	3266.8	3330.8
	2938.0	2922.4	2941.6	2942.6	NA	3082.5
	2915.8	2913.6	2917.9	2907.7	2902.7	3041.7
	1594.8	1594.5	1593.6	1417.2	1589.4	2987.1
	1415.2	1414.8	1415.3	1420.0	1413.7	2950.0
	1378.7	1375.9	1380.5	1377.8	NA	2800.0
	1321.6	1321.5	1322.0	1323.7	1324.1	2741.2
	1092.3	1091.0	1092.3	1141.8	NA	1649.3
	1037.7	1036.1	1038.5	1088.3	1037.3	1606.4
	919.7	919.3	919.7	917.0	NA	1581.1
	848.2	847.3	847.1	833.4	NA	1445.5
	NA	NA	NA	NA	NA	1435.3
	NA	NA	NA	NA	NA	1494.0
	NA	NA	NA	NA	NA	1337.6

584

585 **Table 4. Main FTIR transmittance peaks of drug-free films and films containing**586 **250 µg/strip prepared by SC or TIJP.**

587

Sample	SC			TIJP		
	r^2	b	a	r^2	b	a
Zero-order	0.891	2.2	26.7	0.881	2.2	26.7
1st order	0.747	0.05	3.3	0.685	0.05	3.3
Higuchi	0.988	14.4	9.6	0.983	14.0	10.0
Hixson-Crowell	0.997	29.7	6.8	0.996	29.0	6.2

588

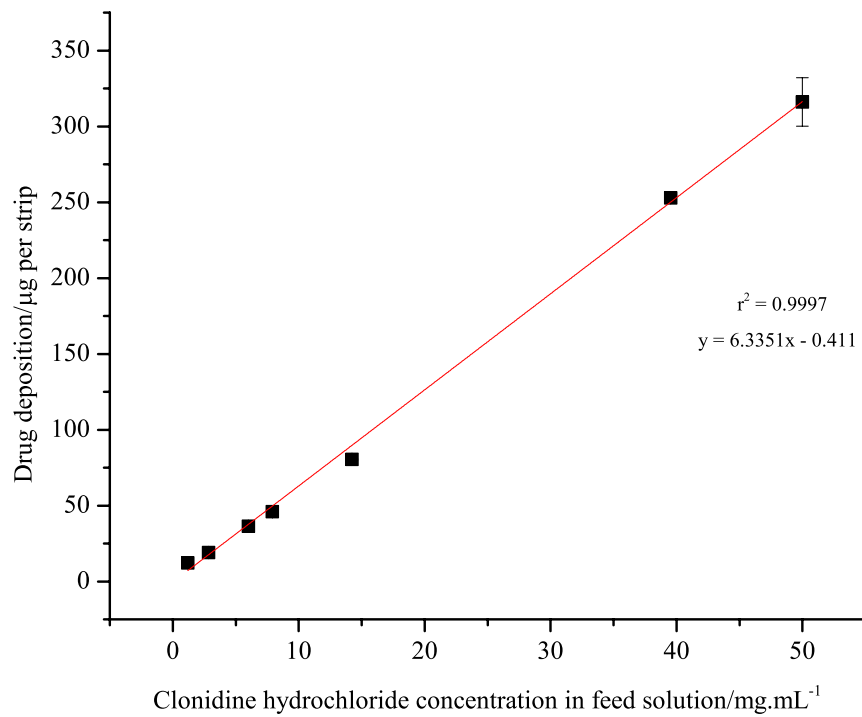
589 **Table 5. Regression values for the dissolution profiles for 250 µg/strip CLN**
590 **films (r^2 is the correlation coefficient, a is the intercept and b is the slope).**

591

592

593

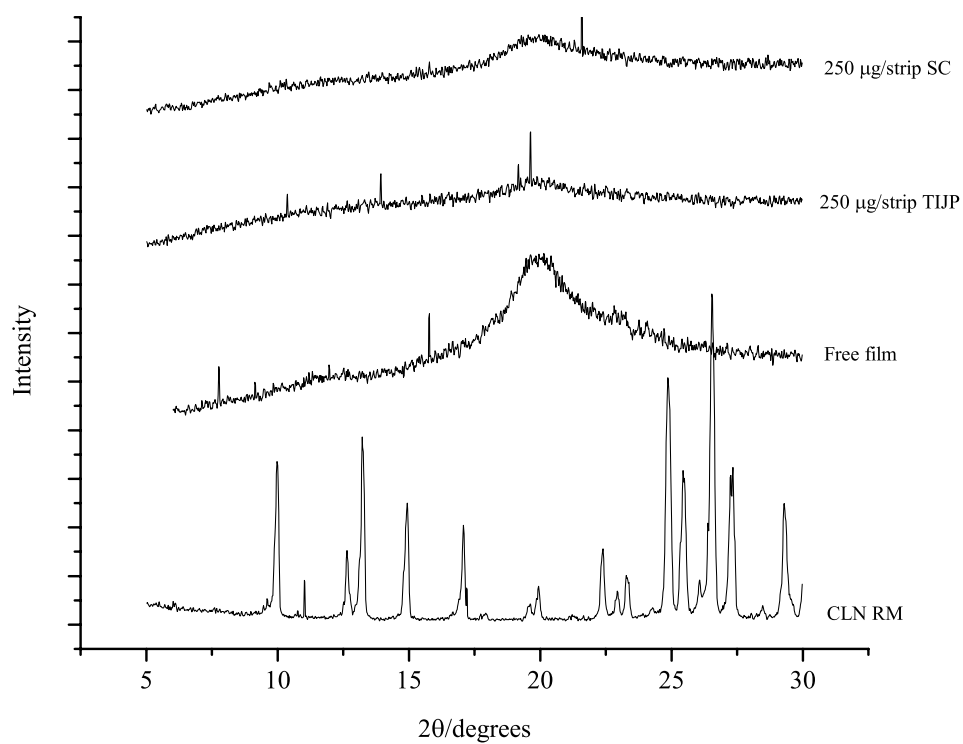
594



595

596 **Figure 1. Amount of clonidine hydrochloride deposited as a function of feed**
597 **solution concentration (some error bars are too small to appear on the graph)**

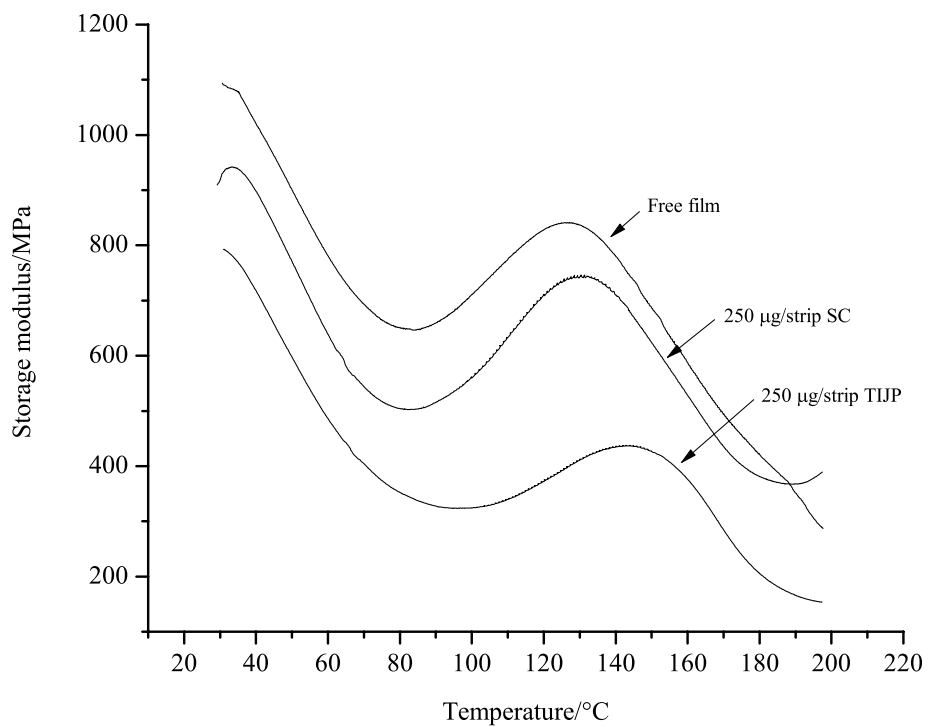
598



600

601 **Figure 2. XRPD patterns of medicated films prepared by SC or TIJP in**602 **comparison to CLN raw material and the free film.**

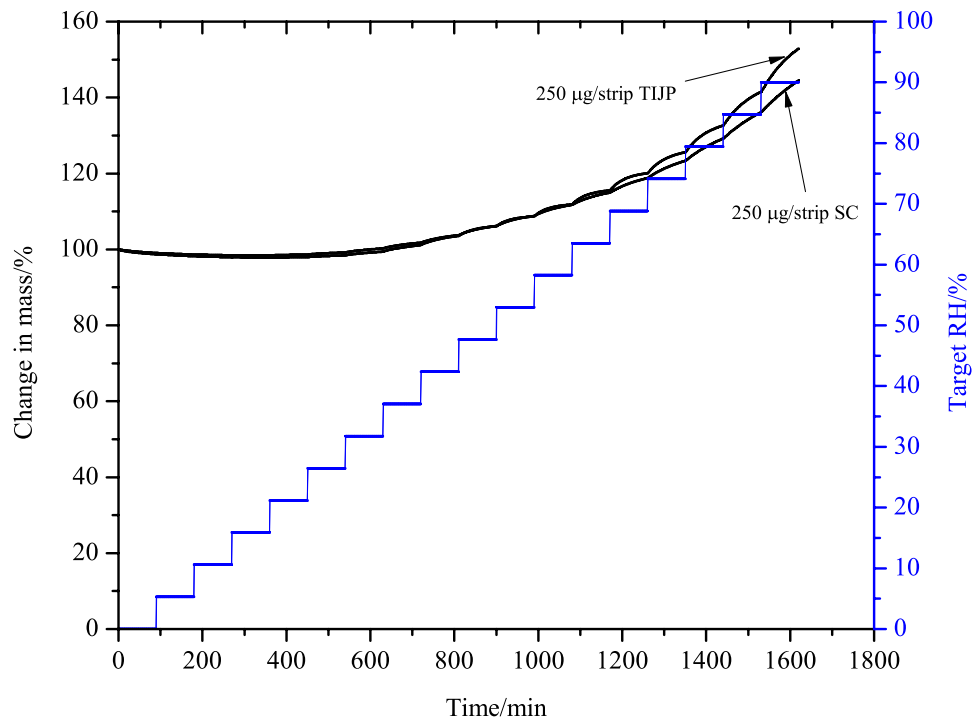
603



604

605 **Figure 3. Storage modulus as a function of temperature for drug-free films and**
 606 **films containing 250µg/strip prepared by SC or TIJP methods.**

607



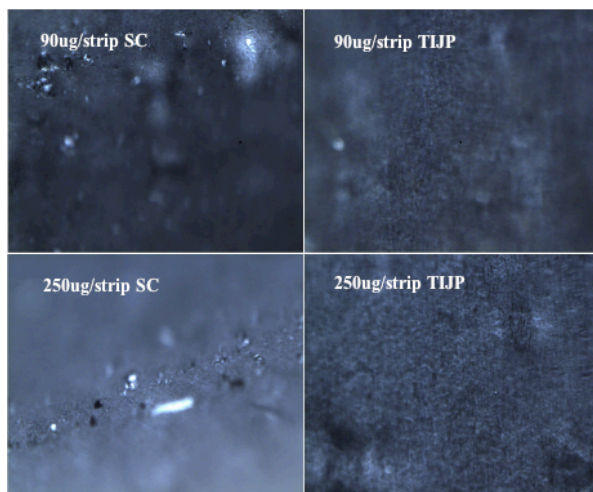
608

609 **Figure 4. DVS results of relative humidity (RH) scan for films containing 250**
 610 **µg/strip prepared by SC or TIJP methods.**

611

612

613



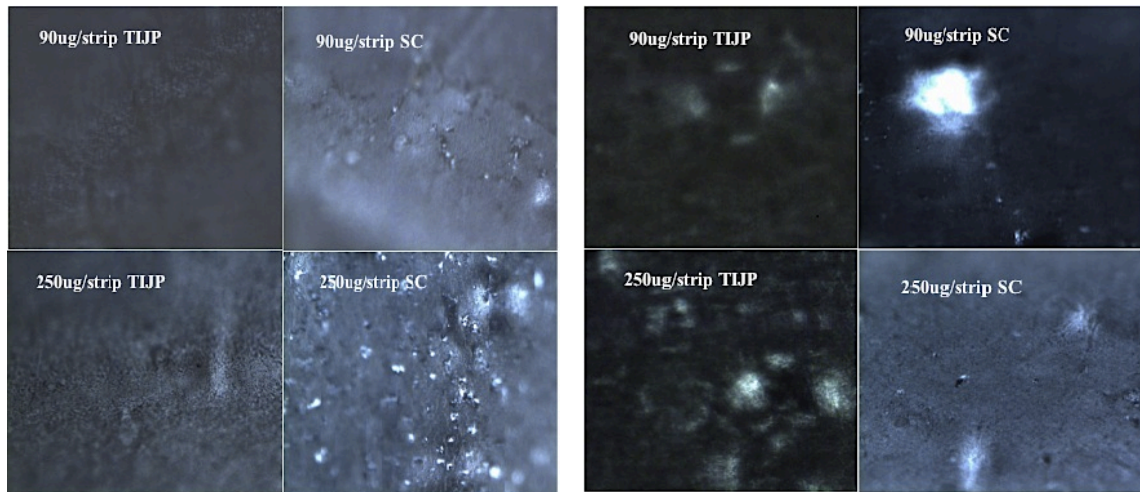
614

615 **Figure 5. PLM images of films after being tested with isothermal constant**
616 **humidity experiments (60°C and 75% RH) in the DMA.**

617

618

619



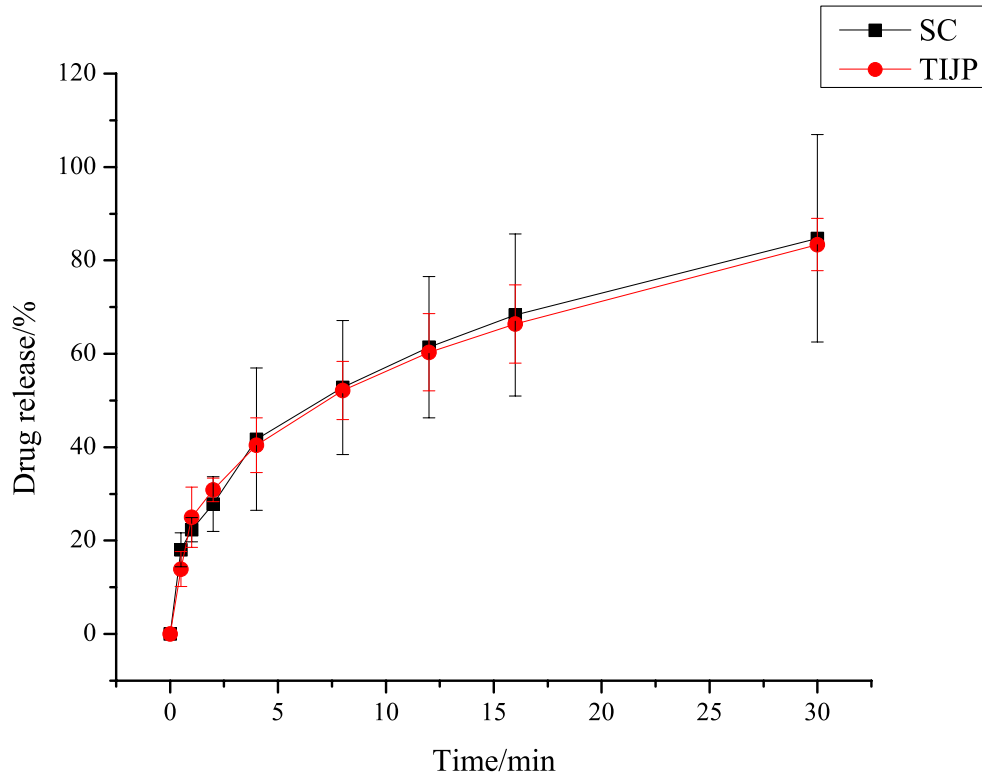
620

621 **Figure 6. PLM images of films subjected to RH scan at 30°C in (left) DVS and**

622 **(right) DMA.**

623

624



625

626 **Figure 7. Dissolution profiles for films containing 250 µg/strip CLN prepared by**
627 **SC or TIJP methods (n = 3).**

628

629